Electronic Supplementary Information (ESI)

Three-dimensional porous MoP@C hybrid as a high-capacity, long-cycle life anode material for Lithium-ion batteries

*Xia Wang, Pingping Sun, Jinwen Qin, Jianqiang Wang, Ying Xiao and Minhua Cao**

Key Laboratory of Cluster Science, Ministry of Education of China, Beijing Key Laboratory of Photoelectronic/Electrophotonic Conversion Materials, Department of Chemistry, Beijing Institute of Technology, Beijing 100081, P. R. China.

* Address correspondence to caomh@bit.edu.cn

Figure contents

Fig. S1 (a,b) Low- and high-magnification FESEM images of MoP@C NPs obtained in the absence of SiO_2 NSPs and (c,d) MoP NPs obtained in the absence of SiO_2 NSPs and citric acid.

Fig. S2 XRD patterns of the as-prepared MoP@C NPs and MoP NPs.

Fig. S3 N_2 adsorption-desorption isotherms of the MoP@C NPs obtained in the absence of SiO_2 NSPs (a) and MoP NPs in the absence of SiO_2 NSPs and citric acid (b).

Fig. S4 Raman spectrum of the as-obtained 3D porous MoP@C hybrid.

Fig. S5 The first five CV curves of the MoP@C NPs (a) and MoP NPs (b).

Fig. S6 The discharge-charge profiles of the 3D porous MoP@C hybrid (a), MoP@C NPs (b) and MoP NPs (c) in a potential window between 0.01 V and 3 V at a current density of 100 mA g^{-1} for the 1st, 2nd, 3rd and 100th cycles.

Fig. S7 The comparison of the specific capacity of this work and those of different metal phosphides in previous reports.

Fig. S8 Equivalent circuit used for simulating the EIS data.

Fig. S9 FESEM image of the 3D porous MoP@C electrode after the 100th cycle at a current density of 100 mA h g^{-1}.

Fig. S10 CV curves of the 3D porous MoP@C hybrid after 100 cycles.

Fig. S11 (a) XRD, (b) FESEM image and (c) cycling performance of the 3D porous WP@C hybrid.

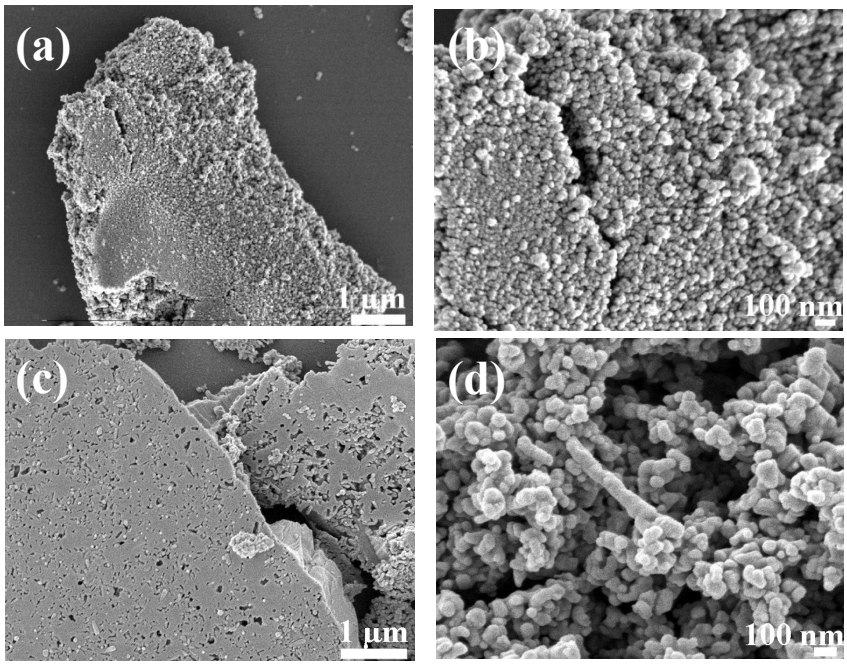

Fig. S1 (a,b)Low- and high-magnification FESEM images of MoP@C NPs obtained in the absence of SiO_2NSPs and (c,d) MoP NPs obtained in the absence of SiO_2 NSPs and citric acid.

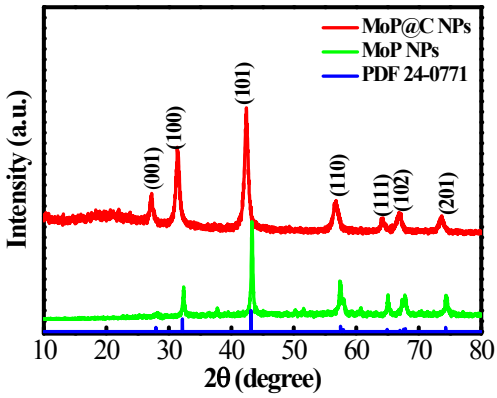

Fig. S2 XRD patterns of the as-prepared MoP@C NPs and MoP NPs.

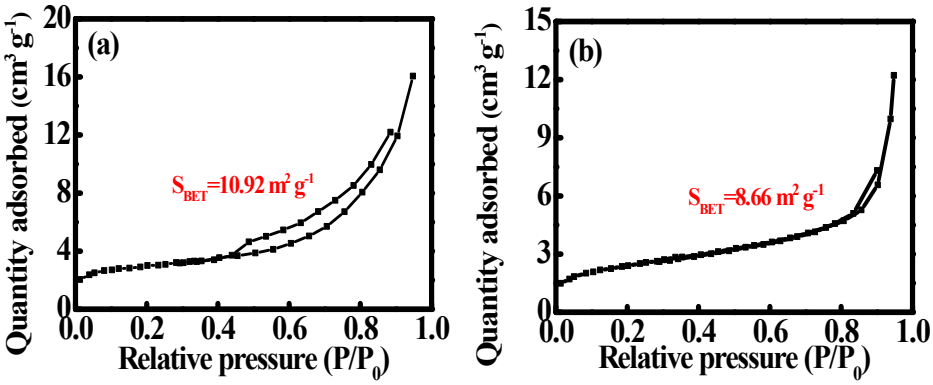

Fig. S3 N_2 adsorption-desorption isotherms of the MoP@C NPs obtained in the absence of SiO_2 NSPs (a) and MoP NPs in the absence of SiO_2 NSPs and citric acid (b).

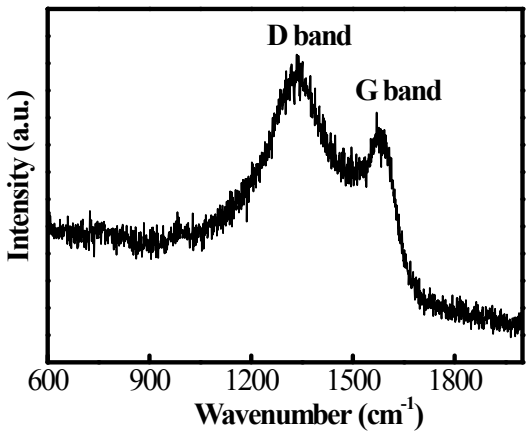

Fig. S4 Raman spectrum of the as-obtained 3D porous MoP@C hybrid.

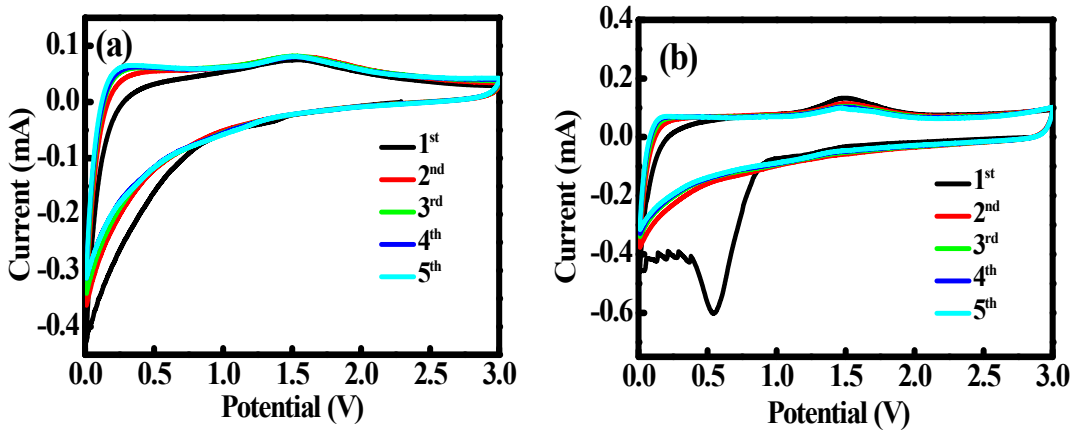

Fig. S5 The first five CV curves of the MoP@C NPs (a) and MoP NPs (b).

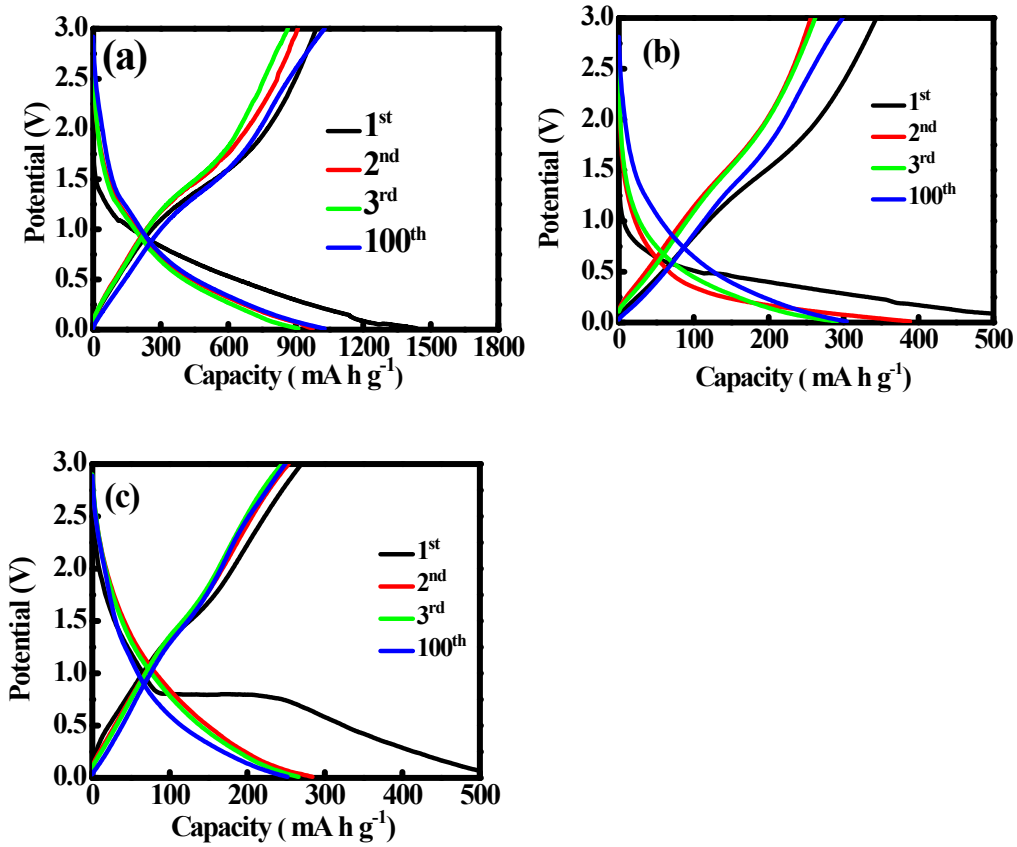

Fig. S6 The discharge-charge profiles of the 3D porous MoP@C hybrid (a), MoP@C NPs (b) and MoP NPs (c) in a potential window between 0.01 V and 3 V at a current density of 100 mA g^{-1} for the 1st, 2nd, 3rd and 100th cycles.

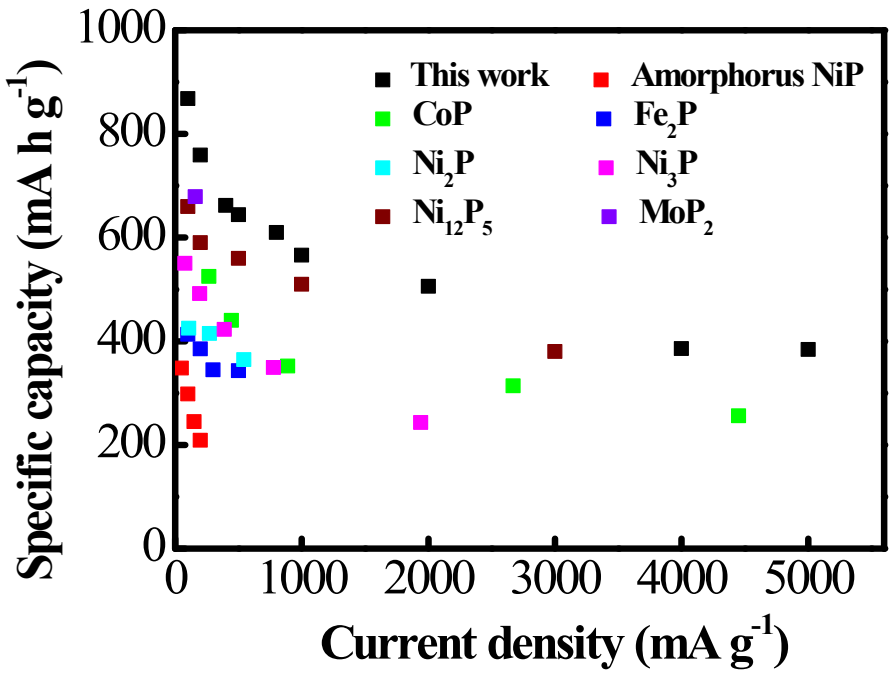

Fig. S7 The comparison of the specific capacity of this work and those of different metal phosphides in previous reports.

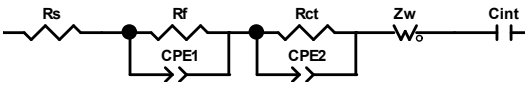

Fig. S8 Equivalent circuit used for simulating the EIS data.

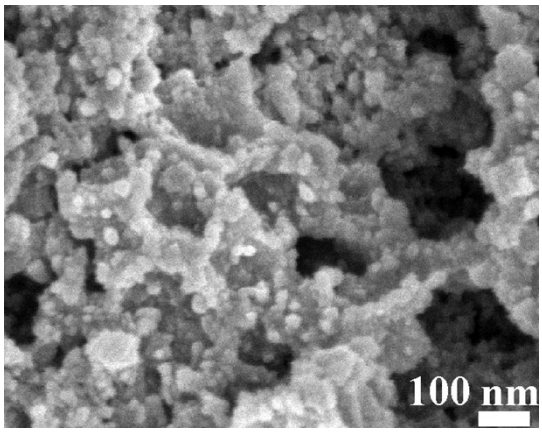

Fig. S9 FESEM image of the 3D porous MoP@C electrode after the 100th cycle at a current density of 100 mA h g^{-1}.

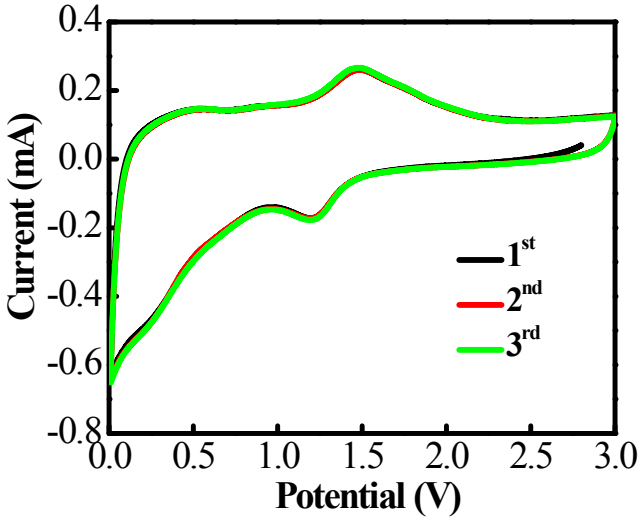

Fig. S10 CV curves of the 3D porous MoP@C hybrid after 100 cycles.

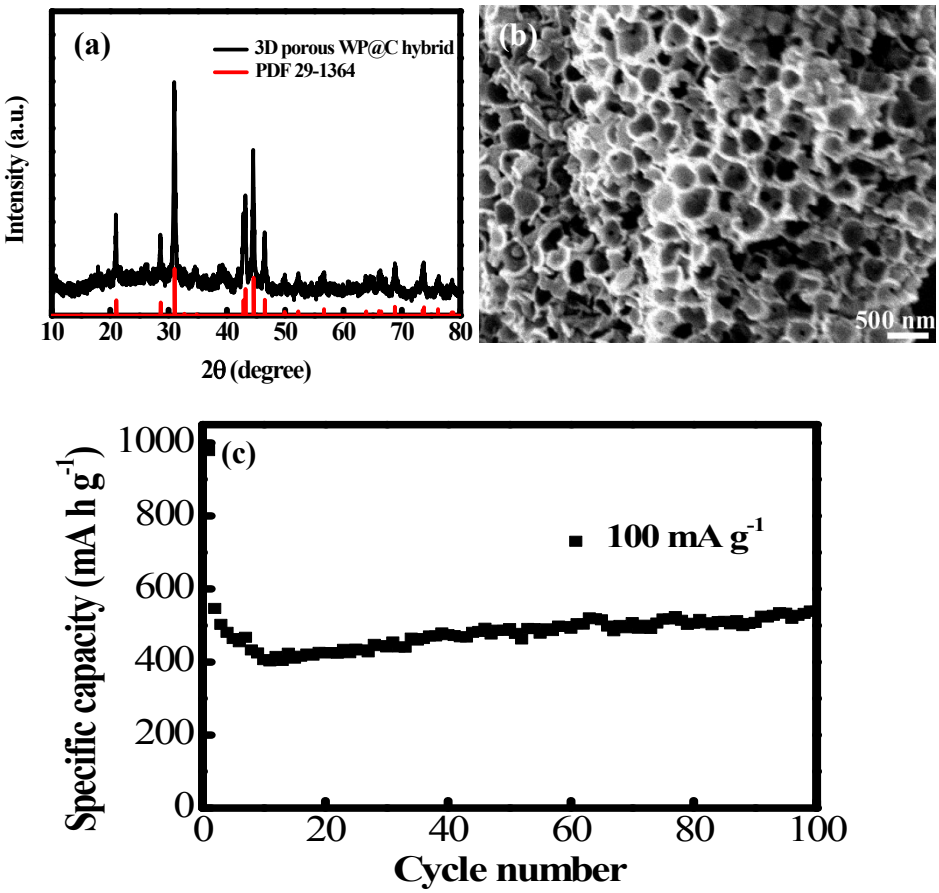

Fig. S11 (a) XRD, (b) FESEM image and (c) cycling performance of the 3D porous WP@C hybrid.

Computational Method

The first-principles calculations based on the density functional theory (DFT) in the current paper were performed by using the plane-wave technique as implemented in the Vienna *ab initio* simulation package (VASP). The ion-electron exchange-correction interactions were treated with thegeneralized gradient approximation (GGA) and projector augmented wave (PAW) methods. A 400 eV cutoff was used for the plane-wave basis set. The exchange-correlation energy is described by the functional of Perdew, Burke, and Ernzerhof (PBE). The geometry optimizations were performed by using theconjugated gradient method, and the Brillouin zone was represented by Monkhorst–Pack with appropriate k-points to ensure the convergence threshold to be 10^{-5}eV in energy and 0.02 eV/Å in force. To investigate the Li diffusion in the supercell, different Li atoms were studied respectively. For better calculation, the initial structure of MoP 2×1×1 supercell with two MoP units was chosen.On the basis of the supercell, Li atoms were inserted from 1 to 4 considering different positions that may be suitable for Li atoms, corresponding 1 MoP unit has 0.5, 1, 1.5, 2 Li atoms, respectively. (We consider the permutation and combination here.) A 2×2×2 supercell after Li insertion with 8 Li_xMoP units is made. During the lithiation, the atomic position and cell structures are fully relaxed simultaneously.

Table S1 Impedance parameters derived using equivalent circuit model for the 3D porous MoP@C, MoP@C NPs, and MoP NPs.

Electrodes	R_s (Ω)	R_f (Ω)	R_{ct} (Ω)	R_{cell} (Ω)
3D porous MoP@C	5.06	23.57	12.95	41.58
MoP@C NPs	3.53	3.98	71.51	79.02
MoP NPs	3.28	5.43	90.67	99.38

Table S2 The basis parameters of Li_xMoP cell (with 8 units) before and after insertion with different Li concentrations

The number of inserted Li	Parameters								
	Position of Li	a /Å	b /Å	c /Å	α /°	β /°	γ /°	V /Å^3	Volume expansion /%
0		12.924	6.462	6.414	90	90	120	463.899	
0.5	Mo-Mo-1	16.984	6.411	6.405	90	90	112.61	643.726	38.76
	P-P-1	16.209	6.493	6.459	90	90	113.56	623.142	34.33
1	Mo-Mo-2	20.725	7.846	6.272	90	90	130.16	779.48	68.03
	P-P-2	19.445	6.621	6.404	90	90	119.75	715.816	54.3
	Mo-P-2	14.220	8.635	6.293	90.36	89.98	114.01	705.827	52.15
	Mo-Mo-1, P-P-1	18.878	6.439	6.471	90	90	119.30	685.966	47.87
1.5	Mo-Mo-2, P-P-1	19.436	6.756	6.653	90	90	110.78	816.731	76.06
	Mo-Mo-2, P-P-1’	20.465	9.251	6.726	90	90	136.50	876.518	88.95
	Mo-Mo-1. P-P-2	19.645	9.123	6.775	90	90	134.36	868.156	87.14
	Mo-Mo-1. P-P-2’	19.484	6.6	6.671	90	90	119.24	748.83	61.42
	Mo-Mo-1, Mo-P-2’	15.768	8.225	9.128	89.83	64.02	121.44	865.603	86.59
	Mo-P-2, P-P-1	14.639	6.335	9.552	72.19	96.24	115.60	760.317	63.9
	Mo-P-2, P-P-1’	14.944	8.161	8.262	74.78	98.65	124.70	799.154	72.27
	Mo-Mo-1, P-P-1, Mo-P-1	18.024	6.531	7.831	90	79.49	111.28	842.36	81.58
	Mo-Mo-1, P-P-1, Mo-P-1’	15.892	7.994	7.948	61.49	118.68	119.18	733.315	58.08
2	Mo-Mo-2, Mo-P-2	15.376	8.867	8.115	89.99	90	125.28	903.18	94.69

	Mo-Mo-1, P-P-1, Mo-P-2	12.838	10.07	8.265	73.17	100.7	105.08	980.829	111.43
	Mo-P-2, P-P-2	15.260	8.719	7.427	67	90.18	117.26	789.88	70.27

Besides, based on the calculated results, the coordinates of the best sites of Li atoms within 8 MoP units are shown in the below table. (Table S3)

Table S3 The coordinates of the best sites of Li atoms within 8 MoP units

sites	Coordinates		
	x	y	z
Li1	0.12653	-0.17759	0
Li2	0.2064	0.18824	0.25
Li3	0.62653	-0.17759	0
Li4	0.70640	0.18824	0.25
Li5	0.12653	0.32241	0
Li6	0.20640	0.68824	0.25
Li7	0.62653	0.32241	0
Li8	0.70640	0.68824	0.25
Li9	0.12653	-0.17759	0.5
Li10	0.20640	0.18824	0.75
Li11	0.62653	-0.17759	0.5
Li12	0.70640	0.18824	0.75
Li13	0.12653	0.32241	0.5
Li14	0.20640	0.68824	0.75
Li15	0.62653	0.32241	0.5
Li16	0.70640	0.68824	0.75